ISSN 0016-7029, Geochemistry International, 2006, Vol. 44, No. 9, pp. 879–895. © Pleiades Publishing, Inc., 2006.
Original Russian Text © B.N. Ryzhenko, N.I. Kovalenko, N.I. Prisyagina, 2006, published in Geokhimiya, 2006, No. 9, pp. 950–966.

Titanium Complexation in Hydrothermal Systems

B. N. Ryzhenko, N. I. Kovalenko, and N. I. Prisyagina

Vernadsky Institute of Geochemistry and Analytical Chemistry, Russian Academy of Sciences, ul. Kosygina 19, Moscow, 119991 Russia

e-mail: ryzhenko@geokhi.ru

Received November 25, 2004

Abstract—The solubility of rutile in aqueous solutions of HCl, HF, H_2SO_4, NaOH, and NaF was determined at 500°C, 1000 bar, and hydrogen fugacity from 8×10^{-12} to 10.3 bar (Mn_3O_4/Mn_2O_3 and Ni/NiO buffers, dissolution of an Al batch weight). The experimentally determined solubility values were used to calculate the constants of the following equilibria at 500°C and 1 kbar pressure: TiO_2(rutile) + H_2O + HCl^0 = $Ti(OH)_3Cl^0$ (pK = 4.89); TiO_2(rutile) + 2HCl^0 = $Ti(OH)_2Cl_2^0$ (pK = 4.69), TiO_2(rutile) + HSO_4^- + H^+ = $Ti(OH)_2SO_4^0$ (pK = 1.98), TiO_2(rutile) + 2HSO_4^- + 2H^+ = $Ti(SO_4)_2^0$ + 2H_2O (pK = –1.50), TiO_2(rutile) + 2H_2O + OH^- = $Ti(OH)_5^-$ (pK = 3.17), TiO_2(rutile) + 2H_2O + 2OH^- = $Ti(OH)_6^{2-}$ (pK = 1.46), TiO_2(rutile) + 2H_2O + F^- = $Ti(OH)_3F^0$ + OH^- (pK = 5.86), TiO_2(rutile) + 2HF^0 = $Ti(OH)_2F_2^0$ (pK = 2.99), and TiO_2(rutile) + 2H_2O + F^- = $Ti(OH)_4F^-$ (pK = 3.69). Based on the results obtained on the composition of volcanic emanations whose Ti concentrations were determined, we evaluated the constants of the equilibria TiO_2(rutile) + H_2O + HCl^0 = $Ti(OH)_3Cl^0$ (pK = 2.74) and TiO_2(rutile) + HSO_4^- + H^+ = $Ti(OH)_2SO_4^0$ (pK = 3.40) at 25°C. The electrostatic model of electrolyte ionization was used to calculate the ionization constants and the Gibbs free energy values for the following Ti species in aqueous fluids at the parameters of postmagmatic processes: $Ti(OH)_3^+$, $Ti(OH)_4^0$, $Ti(OH)_5^-$, $Ti(OH)_6^{2-}$, $Ti(OH)_3F^0$, $Ti(OH)_2F_2^0$, $Ti(OH)_4F^-$, $Ti(OH)_3Cl^0$, $Ti(OH)_2Cl_2^0$, $Ti(OH)_2SO_4^0$, and $Ti(SO_4)_2^0$. As follows from our data on Ti complexation with Cl, F, and SO_4, fluids the most favorable for Ti migration are aqueous acid F-rich solutions with Ti concentrations of no higher than a few fractions of a milligram per kilogram of water.

DOI: 10.1134/S0016702906090047

INTRODUCTION

Titanium, an element of Group 4 of the periodic table, is a transition metal (with a $3d^24s^2$ outer electron shell), atomic number 22, atomic weight 47.90. Naturally occurring Ti consists of a mixture of five stable isotopes: 46 (7.99%), 47 (7.32%), 48 (73.99%), 49 (5.46%), and 50 (5.25%); the known radioactive isotopes are 45 ($T_{1/2}$ = 3.09 h), 51 ($T_{1/2}$ = 5.79 min), and others. The ionization energy (eV) increases in the succession Ti°(6.82) $\mapsto$ Ti^+(13.57) $\mapsto$ Ti^{2+}(27.47) $\mapsto$ Ti^{3+}(43.0) $\mapsto$ Ti^{4+}. Metallic properties are pronounced more clearly in Ti than in other elements of Subgroup 4^b of Group 4 in the periodic table.

The valence of Ti in its compounds with oxygen varies from 2 to 4: TiO, Ti_2O_3, and TiO_2. Compounds of Ti(III) are purple in color [1–3]. Titanium dioxide is amphoteric, and its basic and, particularly, acidic characteristic are pronounced very weakly. Oxides of lower valence display basic properties. $Ti(OH)_3$ is readily oxidized by atmospheric oxygen. Titanium dioxide occurs in three polymorphs: rutile (tetragonal, a = 4.58 Å, c = 2.95 Å), anatase (tetragonal, a = 3.78 Å, c = 9.49 Å), and brookite (orthorhombic, a = 9.16 Å, b = 5.43 Å, c = 5.13 Å). In the presence of water, anatase is transformed into rutile at 375–600°C and 1000–3000 bar. TiO_2 is a chemically inert compound, which is practically insoluble in acids and alkali solutions. TiO_2 can be reduced to lower oxides and a metallic state by heating in an hydrogen flow. Titanium halides and oxyhalides are characterized by a high saturation vapor pressure and are readily hydrolyzed ("smoke" in air). Titanium in its halide compounds has valences of 2, 3, and 4. The salts of Ti acids (Ti-IV) are metatitanates $Me_2^{I}TiO_3$ and $Me^{II}TiO_3$, orthotitanates $Me_2^{II}TiO_4$, and, more rarely, polytitanates with $TiO_2/Me_2^{I}O > 1$. The Ti species stable in aqueous halide solutions is $[TiHl_6]^{2-}$.

Titanium is the fourth most abundant element in the Earth's crust (0.63 wt %) (the first three most abundant elements are Fe, Al, and Mg [3]). Shcherbina [4] noted that Ti, a lithophile element with large ionic radius and high valence, exhibits amphoteric characteristics in naturally occurring minerals. The amphoterism of Ti predetermines the diversity of its modes of occurrence in magmatic minerals. Minerals usually contain Ti in its highest valence and, occasionally, in a valence of III [2]. The major Ti-bearing minerals are ilmenite $FeTiO_3$, rutile TiO_2, perovskite $CaTiO_3$, and sphene $CaTiSiO_5$. Individual Ti minerals usually contain much Ta, Nb, La, V, and other elements. Much Ti is disseminated in the form of admixtures in the crystalline lattices of rock-forming silicates [5].

Deposits of Ti ores belong to three groups: magmatic, sedimentary, and metamorphic. They were produced during certain epochs of ore formation and are grouped into titaniefrous districts and provinces [6]. Magmatic deposits of Ti ores are related to intrusive complexes of basic and alkaline rocks. The orebodies normally do not extend outside the intrusions and were produced by the crystallizing parental magma. The behavior of Ti during magma crystallization is controlled by the initial titanium concentration, the evolving composition of the melt, and the oxygen partial pressure [7]. No Ti deposits are known to be related to either granitoids or typical ultrabasic rocks.

Supergene Ti deposits are formed by the weathering of primary deposits in gabbroids and alkaline rocks and commonly have large reserves of easily processed ores. Metamorphic deposits of Ti ores were produced by the metamorphism of Ti-bearing gabbroid and clayey sedimentary rocks. In the process of metamorphism, titanomagnetite decomposes into ilmenite and magnetite, and ilmenite is further replaced by rutile. Metamorphic complexes are the main source of rutile placers [3].

Titanium is one of the least mobile elements in the hydrothermal process and does not migrate outside the source rocks, so that the altered rocks are commonly neither enriched nor depleted in this element. Titanium is prone to form nonvolatile ionic compounds, and hence, its volatile species do not play any significant role in the migration of this element in geochemical processes. Nevertheless, significant amounts of Ti were detected in groundwaters [8] and in acid thermal waters in the areas of modern volcanic activity [9–11]. The Ti concentration in acidic (pH 1–2) volcanic hydrothermal solutions is sometimes as high as 0.5 mg/l. The element is persistently present in the groundwaters of alkali rock massifs (1–200 μg/l) and in the waters of sulfide oxidation zones.

In the metasomatic process, Ti is redistributed from silicates into its own individual minerals at hydrothermal U deposits [12]. All researchers emphasize that the migration routes of Ti during its extraction from magmatic minerals are relatively short [9].

Titanium concentrations in aqueous solutions systematically vary with variations in the composition of these solutions, particularly their pH and the concentrations of F and organic compounds. The concentrations of Ti increase by factors of 10^3–10^4 in alkaline (to 0.9–2 mg/l at pH > 10) aqueous solutions, a process that can occur only because of Ti complexation. The review of experimental results below on the solubility of Ti-bearing minerals provides a rough idea of the migration characteristics of Ti and its possible speciation in aqueous solutions.

Agapova et al. [12] examined the behavior of Ti in solutions in relation to the genesis of hydrothermal deposits of the Ti–U ore association. The solubility of titanium dioxide powder indicates that the titanium concentration in the aqueous solution is proportional to the concentrations of carbonate and sulfide ions in equilibrium with anatase and reaches $n \times (10^{-4}$–$10^{-3})$ g of Ti per liter. The predominant Ti species in near-neutral solutions is thought to be the $Ti(OH)_2CO_3HS^-$ complex, which gives way to the $Ti(OH)_3(CO)_3(HS)^{2-}$ complex in more alkaline (pH 7.0–8.3) solutions.

The technique of weight loss was employed in [13] to examine the rutile solubility in KF and NH_4F solutions. These researchers arrived at the conclusion that acidic and weakly alkaline solutions at 225–400°C are dominated by the $Ti(OH)_2F_4^{2-}$ complex, and the predominant complex in alkaline solutions at 400–450°C is $Ti(OH)_4F_2^{2-}$, with the Ti solubility independent of pressure within the pressure range of 400–1000 bar.

Oxygen buffers were used in [14, 15] for determining the rutile solubility, which was concluded to be independent of oxygen fugacity and temperature within the temperature range in question (400–700°C). These authors indicated a dependence of rutile solubility on the HCl, HF, and KF concentrations and demonstrated that the characteristics of Ti in hydrothermal solution can be controlled by the concentrations of F and Cl in these solutions and by their pH.

The lower limit of the Ti migration ability at temperatures of 400–700°C and a pressure of 1000 bar is determined by Ti migration in the form of the $Ti(OH)_4^0$ hydroxycomplex and is equal to 1×10^{-6} m. The Ti concentration in the solutions increases with increasing F and Cl concentrations. At equal concentrations of halides, the migration ability of Ti is higher in fluoride than in chloride solutions and is higher in acidic solutions than in neutral and alkaline ones. It is thought that the formation of the $Ti(OH)_4(F,Cl)^-$, $Ti(OH)_3(F,Cl)^0$, and $Ti(OH)_2(F,Cl)_2^0$ hydroxide–fluoride complexes controls the mobility of Ti at HF concentrations within the range of 0.001–0.02 *m* and HCl concentrations within the range of 0.1–0.25 *m*.

The solubilities of rutile and anatase in 1 M NaCl solution were compared in [16]. The solubilities at 200

and 300°C and the saturated pressure of water vapor are equal to, respectively, 1.68×10^{-4} and 2.07×10^{-4}% for anatase and 1.33×10^{-4} and 1.57×10^{-4}% for rutile.

In order to assay the role of titanium in magmatic processes within subduction zones, the solubility of rutile in water was examined using the weight loss method, and the Ti mobility in supercritical aqueous fluids was evaluated within the temperature range of 750–1200°C and pressures of 1–36 GPa [17, 18]. The temperature and baric dependence of rutile solubility udder these parameters has the form $\log m_{Ti} = -7049(\pm 475)/T - 0.589(\pm 0.073)*P/T + 5.14$.

It is known from studies dealing with crystal growth that intense TiO_2 recrystallization occurs in fluoride solutions (7–10% KF and NaF solutions) [19–22]. Published experimental results on the solubility of Ti (IV) oxides are presented in Table 1.

EXPERIMENTAL

The task of our research was formulated as the experimental determination of the solubility of rutile in HCl, HF, NaF, NaOH, and H_2SO_4 solutions at hydrogen fugacity within the range of 8×10^{-12} to 10.3 bar. A dependence of rutile solubility on the concentrations of ligands in an aqueous solution can be utilized to clarify the speciation of Ti in supercritical fluids within a broad range of hydrogen fugacity values and then quantify the conditions under which Ti can migrate in postmagmatic processes.

Examination of rutile used in the experiments. The solubility of TiO_2 was determined using pinkish yellow and black rutile boules that had been grown in melt (they were provided to us by courtesy of M.L. Barsukova and E.I. Efremova of the laboratory headed by V.A. Kuznetsov at the Institute of Crystallography, Russian Academy of Sciences). The color of the material seems to have been controlled by the oxygen regime when the crystals were grown. X-ray diffraction data indicate that the samples were made up of rutile alone. Its refined unit cell parameters (A.M. Bychkov) are as follows: $a = b = 4.5964$ (14) Å and $c = 2.9598$ (11) Å for pinkish rutile; $a = b = 4.5957$ (15) Å and $c = 2.9588$ (11) Å for black rutile; and $a = b = 4.5933$ Å and $c = 2.9592$ Å for a rutile standard (ASTM no. 21-1276, year 1969). Hence, the unit cell parameters of our samples coincided within the error of the X-ray diffraction determinations. Neither stoichiometric deviations nor foreign phases were detected. The homogeneity of the crystals was confirmed by their microprobe analyses (on a Cameca microprobe, analyst V.G. Senin). The chemical composition of the rutile sample (analyst I.A. Roshchina) is presented in Table 2. The mineral contains 98.61 (pink rutile) and 97.73% (black rutile) TiO_2.

Methods used for Ti analysis in aqueous solutions. To determined the Ti concentration in aqueous solutions, we needed highly sensitive and accurate analytical techniques. The photometric (on a SF 16 spectrophotometer) determination of minor Ti concentrations with Tichromine (on a wave of 470 nm) and diantipirylmethane (DAM) (385 nm) allowed us to determine

Table 1. Results of preexisting experimental measurements of the rutile solubility (literature data)

Temperature, pressure	Solid phase	Solvent	Ti concentration in solution, *m*	Method	Reference
400°C, 1 kbar	Rutile	KF	$n \times 10^{-4}$–10^{-3}	Weight loss	12
450°C, 1.4 kbar					
225°C, 600 bar	Rutile	NH_4F	$n \times 10^{-4}$–10^{-1}	″	12
400°C, 400 bar					
200°C, 100 bar	Anatase	CO_2, H_2S, SO_4	$n \times 10^{-5}$–10^{-4}	Sampling	11
200–700°C, 1 kbar	Rutile	H_2O	$n \times 10^{-7}$	″	14
400–700°C, 1 kbar	Rutile	HF	$n \times 10^{-6}$–10^{-2}	Two-ampoule method with an oxygen buffer	14
400–700°C, 1 kbar	Rutile	HCl	$n \times 10^{-6}$–10^{-3}	″	14
200 °C, sat. vap.	Anatase	1*m* NaCl	$(3.51 \pm 0.34) \times 10^{-5}$	Sampling	15
200°C, sat. vap.	Rutile	1*m* NaCl	$(2.78 \pm 0.45) \times 10^{-5}$	″	15
300°C, sat. vap.	Anatase	1*m* NaCl	$(4.32 \pm 0.10) \times 10^{-5}$	″	15
300°C, sat. vap.	Rutile	1*m* NaCl	$(3.28 \pm 0.38) \times 10^{-5}$	″	15
1000°C, 29.3 kbar	Rutile	H_2O	$(1.880 \pm 0.1) \times 10^{-2}$	Weight loss	16, 17
1100°C, 10 kbar	Rutile	H_2O	$(2.38 \pm 1.0) \times 10^{-1}$	″	16, 17

Table 2. XRF analyses of rutile samples synthesized in the experiments (analyst I.A. Roshchina)

Component	SiO_2	TiO_2	Al_2O_3	Fe_2O_3	CaO	Na_2O	K_2O	P_2O_5	Cl	Cr	Ni	Total
Yellow rutile	0.73	98.61	–	0.24	0.05	0.22	0.03	0.04	0.09	–	–	100.01
Black rutile	1.03	97.73	0.16	0.32	0.07	0.25	–	0.03	0.12	0.18	0.10	99.99

Ti concentrations near the limit of rutile solubility (0.2 μg Ti/ml) [23, 24]. Because of this, the Ti determinations were carried out by the atomic emission technique with inductively coupled plasma (ICP-AE) on an ICAP-9000 (United States) 48-collector spectrometer. We selected optimal conditions for Ti analysis and introduced correlation coefficients for the analytical signal and background correction. The calibration was conducted on a reference solution with a Ti concentration of 10 μg/ml. The minimal determinable Ti concentration was 0.01 μg of Ti/ml.

Species with Ti in lower valences were determined in the experimental solutions using a qualitative reaction with ammonium molybdate. Under the effect of trivalent Ti (which is a weak reducer), Mo was reduced to its pentavalent state and turned the solution to a pale blue color.

Preparatorily to the experiments aimed at assaying the rutile solubility in HF solutions, we conducted a methodological research with standard solutions. A set of standard solutions with Ti concentrations from 1 to 10 μg Ti/ml and sulfuric acid was evaporated in a water bath to remove F. The anhydrous residue was washed out with 2N solution of HCl. No Ti losses were detected. Both methods (photometry and ICP-AE) yielded consistent results.

Experimental determination of rutile solubility. Platelets (0.1–0.2 g) prepared of the pink rutile and electrolyte solutions (HCl, HF, NaF, NaOH, and H_2SO_4) were placed in gold ampoules ($8 \times 0.1 \times 70$ mm) permeable to hydrogen. The ampoules were welded, weighed, and put into autoclaves made of temperature-resistant steel and containing buffer mixtures in their bottom parts. The autoclaves were filled with calculated amounts of water that would have ensured a pressure of 1000 bar at 500°C. The closed autoclaves were placed into a gradientless furnace with a nichrome heater. The experiments lasted for 10–14 days. Upon their completion, the autoclaves were quenched, and the ampoules were extracted from them, weighed, and opened. The solutions from the ampoules were diluted with 2 N HCl solution and analyzed. It is interesting to mention that the pink rutile preserved its color in the experiments at a high oxygen fugacity (with the Mn_2O_3/MnO_2 buffer) but became black in the experiments under more reduced conditions (with the Ni/NiO and Al/Al_2O_3 buffers). We managed to transform black rutile into pink rutile in experiments with the Mn_2O_3/MnO_2 buffer.

DETERMINING RUTILE SOLUBILITY

In compliance with the task of elucidating the speciation of Ti in lower valence states, we noted the change in the rutile color depending on the oxygen fugacity of the buffers used in the experiments. Rutile after these experiments reversibly changed its color from pink in experiments with the Mn_2O_3/MnO_2 buffer to black in experiments with the Ni/NiO buffer and an Al charge. It is interesting that the color of rutile in experiments with the Mn_2O_3/MnO_2 buffer also depended on the pH of the aqueous solution. Pink rutile remained stable in diluted HF solutions (<0.27 *m*) but became pale gray in experiments with a 1.37 *m* HF solution and gray in experiments with a 2.74 *m* HF solution. The intense black color of rutile in experiments with reducing buffers testifies to the appearance of oxygen vacancies in the rutile crystalline structure and the partial reduction of Ti(+4) to Ti(+3). The presence of Ti(+3) was documented in synthetic and natural Ti-bearing micas of violet color. The change in the color is reportedly related to the intense interaction of the Ti(+4) and Ti(+3) ionic pair. Hence, Ti(+3) likely occurs in the system in the solid phase.

No Ti(+3) was found in the aqueous solution after the experiments (reaction with ammonium molybdate), even in the experiments with the reduction potential increased to 10 bar hydrogen (Al batch weight, experiments lasting for up to 20 days), possibly due to the ability of Ti(+3) to be easily oxidized in air.

SYSTEMS TiO_2 (RUTILE)–HCl, HF, H_2SO_4, NaOH, OR NaF SOLUTION AT 500°C AND 1000 BAR

System rutile–aqueous HCl solutions (Table 3). The rutile solubility determined at 500°C and 1000 bar in aqueous HCl solutions (0.01–0.1 *m*) testifies that the rutile solubility was near the detection limit of the analytical techniques (0.01 μg of Ti per ml of solution) for all of the redox buffers. The Ti concentration increased from $n \times 10^{-6}$ *m* to $n \times 10^{-4}$ *m* when the HCl concentration was increased from 0.3 to 3 *m* (Fig. 1). It should be mentioned that the rutile solubility at the Ni/NiO and Al/Al_2O_3 buffers was one order of magnitude lower than that determined by Purtov and Kotel'nikova [15] under analogous experimental conditions (Fig. 1). Analyses of the inner surface of the platinum ampoules on a microprobe did not reveal the presence of any Ti-

bearing phases; i.e., no precipitate was formed during quenching. The reasons for these discrepancies are still uncertain.

We did not detect any changes in the rutile solubility at an increase in the redox potential from the Ni/NiO to the Al/Al_2O_3 buffer (Table 4). Neither did we identify Ti(+3) in the aqueous solution after the experiments, perhaps, because of its insufficient concentration.

System rutile–aqueous HF solutions (Table 5). For all of the redox buffers, the solubility of rutile in HF solutions (with HF concentrations of >0.027 *m*) was higher than the sensitivity of the analytical technique (0.01 μg of Ti/ml). When the HF concentration was increased (within the range of 0.027–2.74 *m*), the Ti concentration in the aqueous solution after the experiments increased within the range of $n \times 10^{-6}$ to $n \times 10^{-2}$ *m* (Fig. 2). At an HF concentration of >1 *m*, the rutile solubility somewhat increased with increasing redox potential of the buffers. As in the experiments with HCl, no Ti(+3) was detected in the aqueous solution after the experiments. The comparison of the rutile solubility in HCl and HF solutions indicates that the complexation ability of acid fluoride solutions is notably stronger (Fig. 3), a fact also noted by other researchers (Table 1).

The evaluations of the rutile solubility allowed us to calculate the constants of the equilibria at 500°C and 1 kbar. Aqueous solutions of HCl and HF under these parameters are dominated by neutral associated species of these acids (HCl^0 and HF^0). The fractions of the associated species can be quantified by calculating the complexation of the aqueous solution of the acid under the experimental *P–T* parameters. These results are listed in Tables 6 and 7 as HCl^0 and HF^0 molality. The Ti concentration of $Ti(H_2O)$ (assumed to be equal to 1×10^{-6} *m*, Fig. 3) in pure water was subtracted from the experimentally determined Ti concentration in the aqueous solution.

As was mentioned above, rutile dissolves in pure water predominantly in the form of $Ti(OH)_4^0$, and hence, the probable reactions forming hydroxo–halogen complexes can be written in the form of OH^- substitution for Cl^- and F^-,

$$TiO_2(\text{rutile}) + nHCl^0 = Ti(OH)_{4-n}Cl_n + (n-2)H_2O, \quad (1)$$

$$TiO_2(\text{rutile}) + nHF^0 = Ti(OH)_{4-n}F_n + (n-2)H_2O. \quad (2)$$

The prevalence of any of these reactions (the value of *n* in the equations of the reactions) in HCl and HF solutions was evaluated from the constancy of the constant at variations in the concentrations of the acids. As can be seen from Table 6, the constant of reaction (2) remains unchanged at $n = 2$ for the $Ti(OH)_2Cl_2^0$ complex only at the three last points (1.0–3.0 *m* HCl). Then the probable predominant complex at concentrations of <1 *m* (the first two points, 0.3 and 0.5 *m* HCl) is $Ti(OH)_3Cl^0$. If both species are contained in equal concentrations at the boundary of HCl concentrations at the

Table 3. Rutile solubility in HCl solutions at 500°C and 1000 bar [Ti(aq), $m \times 10^{-4}$]

Initial HCl concentration (*m*)	Ni/NiO buffer	Al charge	Assumed averaged solubility value ($m \times 10^4$)
	hydrogen fugacity 1.74 bar	hydrogen fugacity 10.3 bar	
H_2O	<0.01	<0.01	0.01
0.2	–	0.014	0.014
0.3	0.042	0.030	–
0.3	0.030	0.028	–
0.3	–	0.021	–
0.3	–	0.027	–
0.3	–	0.027	0.029
0.5	0.176	0.115	–
0.5	0.248	0.185	–
0.5	0.0075	0.266	–
0.5	–	0.056	–
0.5	–	0.054	–
0.5	–	0.071	0.109
1.0	0.22	0.288	–
1.0	0.194	0.180	–
1.0	0.286	0.214	–
1.0	0.274	0.227	0.235
2.0	0.859	0.922	–
2.0	0.634	1.12	–
2.0	–	0.934	–
2.0	–	0.804	–
2.0	–	0.846	–
2.0	–	1.19	–
2.0	–	0.803	0.90
3.0	0.95	3.47	2.21

Table 4. Comparison of rutile solubility at 500°C, 1000 bar, and variable hydrogen fugacity (log*m*Ti)

HCl, *m*	Mn_2O_3/MnO_2 $fH_2 = 8 \times 10^{-12}$ bar [15]	Ni/NiO $fH_2 = 1.74$ bar	Al/Al_2O_3 $fH_2 = 10.3$ bar
0.3	–	–5.39	–5.54
0.5	–4.42	–4.76	–4.82
1.0	–3.72	–4.66	–4.54
2.0	–	–4.96	–4.99

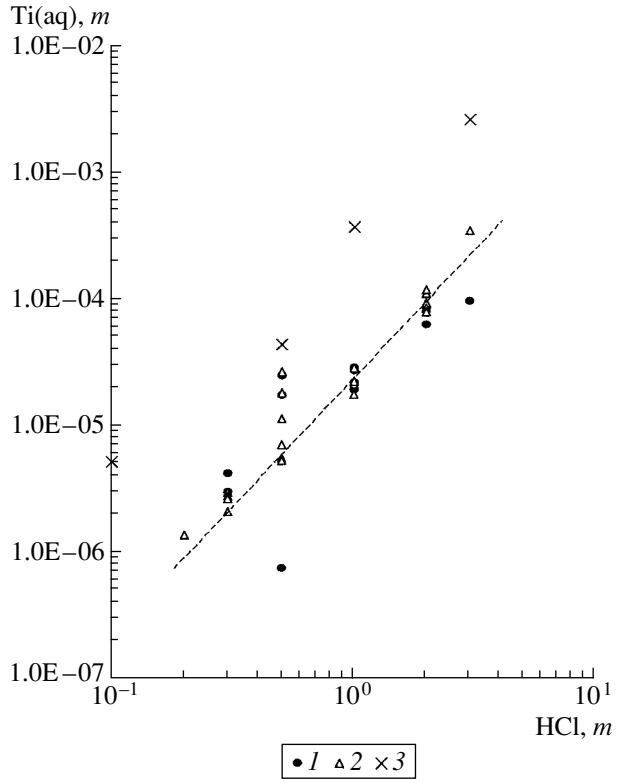

Fig. 1. Rutile solubility in HCl solutions at 500°C, 1000 bar, and the Mn_2O_3/MnO_2, Ni/NiO, and Al ⟶ Al_2O_3 buffers. (*1*) Ni/NiO and Mn_2O_3/MnO_2 buffers; (*2*) Al charge; (*3*) results from [15].

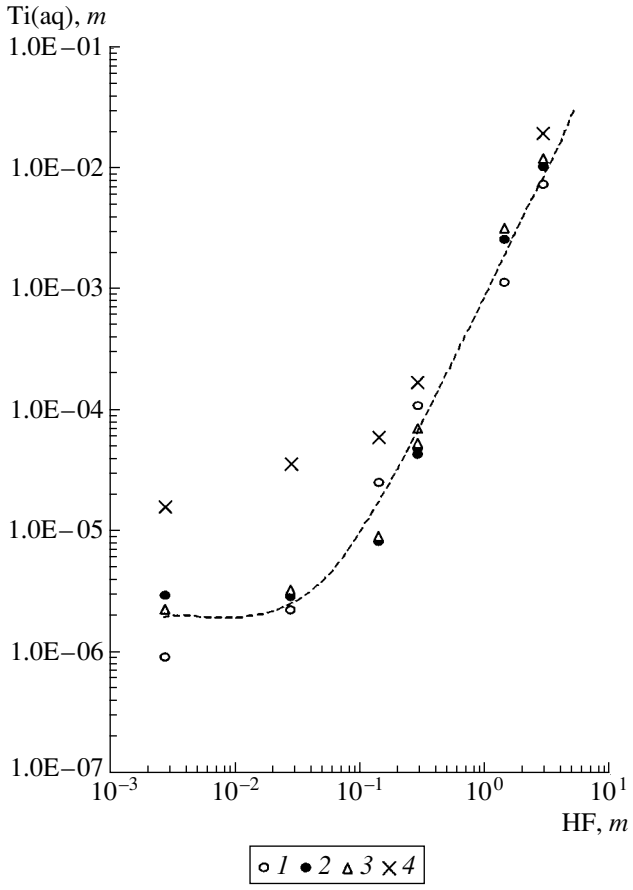

Fig. 2. Rutile solubility in HF solutions at 500°C, 1000 bar, and the Ni/NiO and Al ⟶ Al_2O_3 buffers. (*1*) MnO_2/Mn_2O_3 buffer; (*2*) Ni/NiO buffer; (*3*) Al batch weight; (*4*) results from [14].

point of 1.0 *m*, then the Ti solubility in 1.0 *m* HCl solution should be regarded as equally determined by both of the species, and then $K = 1.29 \times 10^{-5}$, p$K = 4.89$ at $n = 1$ and $K = 20.3 \times 10^{-6}$, p$K = 4.69$ at $n = 2$. The value of the constant of reaction (1) at *n* equal to 3 and 4 obviously decreases with increasing HCl concentration. In calculating the equilibrium constants, we assumed that the activity coefficients were equal to one.

Table 5. Rutile solubility in HF solutions at 500°C and 1000 bar [Ti(aq), $m \times 10^{-4}$]

Initial HF concentration (*m*)	MnO_2/Mn_2O_3 buffer Hydrogen fugacity 8×10^{-12} bar	Ni/NiO buffer Hydrogen fugacity 1.74 bar	Al charge Hydrogen fugacity 10.3 bar
H_2O	0.01	0.01	0.01
0.0027	0.0093	0.030	0.023
0.027	0.0223	0.0294	0.0332
0.137	0.256	0.0812	0.0921
0.274	1.08	0.488	0.534
0.274	–	0.433	0.711
1.37	11.1	25.2	31.3
2.74	71.2	99.8	117

For reaction (2), an increase in the HF concentration is associated with a monotonic increase in the constant at $n = 1$ [the $Ti(OH)_3F^0$ complex] and with its decrease at $n = 3$ and 4. The solubility value is less variable at $n = 2$, i.e., for the $Ti(OH)_2F_2$ complex, whose $K = 1.01 \times 10^{-3}$ and p$K = 2.99$ (Table 7).

System rutile–aqueous H_2SO_4 solutions (Table 8). The qualitative reaction for Ti^{+3} identification did not yield a positive result. Nevertheless, the rutile crystals in equilibrium with the aqueous solution were noted to become paler, a phenomenon that takes place when the redox potential of the system increases, and the color of rutile crystals changes from black to pinkish gray. As can be seen in Table 8 and Fig. 4, the rutile solubility is at a minimum, near the detection limit of the analytical technique, at the initial H_2SO_4 concentrations of 0.01–0.2 *m*. As the H_2SO_4 concentration was increased to

Table 6. Calculation of the constant of the equilibrium TiO_2(rutile) + $n HCl^0$ = $Ti(OH)_{4-n}Cl_n$ + $(n-2)H_2O$ at 500°C and 1000 bar ($K \times 10^{-6}$)

Initial HCl concentration (m)	HCl^0 (m)	$\frac{Ti(aq) - Ti(H_2O)}{HCl^0}$	$\frac{Ti(aq) - Ti(H_2O)}{(HCl^0)^2}$	$\frac{Ti(aq) - Ti(H_2O)}{(HCl^0)^3}$	$\frac{Ti(aq) - Ti(H_2O)}{(HCl^0)^4}$
First approximation					
0.3	0.287	6.62	23.1	80.4	280
0.5	0.482	20.5	42.5	88.4	183
1.0	0.972	23.1	23.8	24.5	25.2
2.0	1.95	45.6	23.4	12.0	6.16
3.0	2.94	74.8	25.5	8.66	2.94
Second approximation					
0.3	0.287	6.62	–	–	–
0.5	0.482	20.5	–	–	–
1.0	0.972	11.6	11.9	–	–
2.0	1.95	–	23.4	–	–
3.0	2.94	–	25.5	–	–

Note: $K = 12.9 \times 10^{-6}$, $pK = 4.89$ for the reaction TiO_2(rutile) + H_2O + HCl^0 = $Ti(OH)_3Cl^0$; $K = 20.3 \times 10^{-6}$, p$K = 4.69$ for the reaction TiO_2(rutile) + $2HCl^0$ = $Ti(OH)_2Cl_2^0$.

Table 7. Calculation of the constant of the equilibrium TiO_2(rutile) + $n HF^0$ = $Ti(OH)_{4-n}F_n$ + $(n-2)H_2O$ at 500°C and 1000 bar, $K \times 10^{-4}$

$HF(m) = HF^0$	Ti(aq), $m \times 10^{-4}$	$\frac{Ti(aq) - Ti(H_2O)}{HF^0}$	$\frac{Ti(aq) - Ti(H_2O)}{(HF^0)^2}$	$\frac{Ti(aq) - Ti(H_2O)}{(HF^0)^3}$	$\frac{Ti(aq) - Ti(H_2O)}{(HF^0)^4}$
0.137	0.0143	0.971	7.09	51.7	378
0.274	0.65	2.34	8.52	31.1	114
1.37	22.5	16.4	12.0	8.75	6.39
2.74	96.0	35.0	12.8	4.67	1.70

Note: $K = 10.1 \times 10^{-4}$, p$K = 2.99$ for the reaction TiO_2(rutile) + $2HF^0$ = $Ti(OH)_2F_2$.

0.5 m, the rutile solubility increased to 2.4×10^{-5} m. The predominant species in an aqueous H_2SO_4 solution at 500°C and 1000 bar are associated particles: the HSO_4^- ion and the $H_2SO_4^0$ neutral species. By analogy with reactions of rutile dissolution in HCl and HF solutions, the dissolution of this mineral in H_2SO_4 can be regarded as a reaction of OH^- substitution for SO_4^{2-}.

$$TiO_2(\text{rutile}) + nHSO_4^- + nH^+ = Ti(OH)_{4-2n}(SO_4)_n + nH_2O. \quad (3)$$

Table 9 reports the calculated constant of reaction (3). For the points at 0.2–0.5 m H_2SO_4, the equilibrium constant remains unchanged with increasing H_2SO_4 concentrations at $n = 2$. The $Ti(OH)_2SO_4^0$ ($n = 1$) complex should be predominant at points corresponding to lower concentrations of H_2SO_4, i.e., at points with H_2SO_4 concentrations of 0.1 m or lower in the experiments.

Table 8. Rutile solubility in H_2SO_4 solutions at 500°C, 1000 bar, and the Ni/NiO buffer

Initial H_2SO_4 concentration (m)	Experimentally determined value of the Ti concentration ($m \times 10^{-4}$)	Averaged Ti solubility value ($m \times 10^{-4}$)
0.01	0.0264	0.0282
	0.0300	
0.1	0.0258	0.0209
	0.0160	
0.2	0.0258	0.0284
	0.0310	
0.3	0.061	0.061
0.4	0.127	0.122
	0.116	
0.5	0.265	0.241
	0.217	

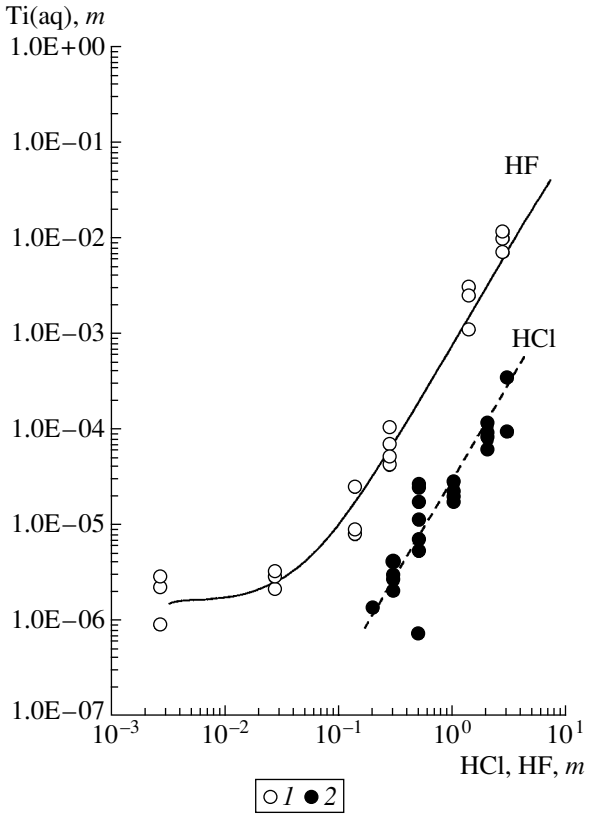

Fig. 3. Comparison of rutile solubility in (*1*) HF and (*2*) HCl solutions at 500°C and 1000 bar.

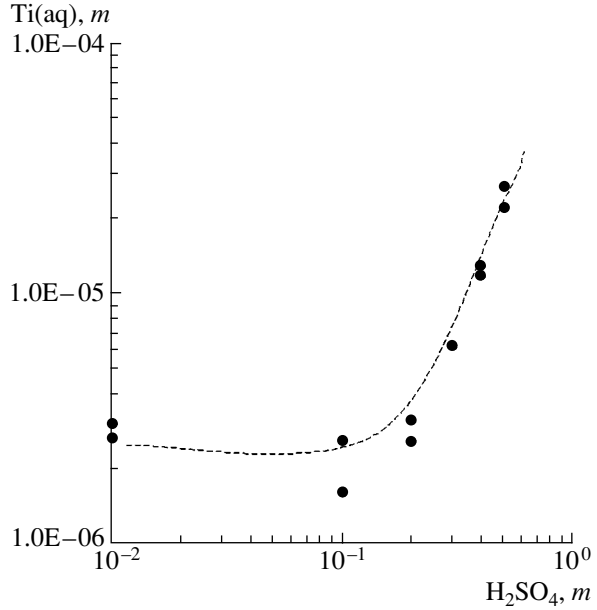

Fig. 4. Rutile solubility in H_2SO_4 solutions at 500°C, 1000 bar, and the Ni/NiO buffer.

The threefold decrease in K with increasing H_2SO_4 concentration at $n = 3$ casts doubt on the predominance of the $Ti(SO_4)_3^{2-}$ complex. Excluding the point corresponding to 0.2 m H_2SO_4, which is a boundary point for the $Ti(OH)_2SO_4^0$ and $Ti(SO_4)_2^0$ complexes, and the point of 0.01 m, which corresponds to the detection limit of the analytical technique, we obtained $K = 32.5$ and $pK = -1.51$ for equilibrium (3) in a 0.3–0.5 m H_2SO_4 solution at $n = 2$ and $K = 10.5 \times 10^{-3}$ and $pK = 1.98$ for a 0.1 m H_2SO_4 solution at $n = 1$ (Table 9). The activities of the HSO_4^- and H^+ ions were calculated by the HCh computer program (developed by Yu.V. Shvarov) by simulating the speciation of H_2SO_4 at 500°C and 1000 bar. The activity coefficients of the dissolved Ti species were assumed to be equal to one.

System rutile–aqueous NaOH solutions (Table 10). The rutile solubility was determined only for the Ni/NiO buffer (Fig. 5). The quantification of the rutile solubility was complicated by the origin of a white felty phase (Fig. 6) at a NaOH concentration of 0.5 m. At first, these were single white shreds, which then (at increasing NaOH concentrations) tightly enveloped black rutile crystals, with some newly formed crystals precipitating when the solution was removed from the ampoule.

The morphology and chemical composition of the newly formed phases were examined on a Jeol JSM-561LV digitalized scanning microscope equipped with a JED-2300 spectrometer in low vacuum, without sputter coating (analyst A.V. Mokhov, Institute of the Geology of Ore Deposits, Petrography, Mineralogy, and Geochemistry, Russian Academy of Sciences). The X-ray diffraction analysis was conducted (by V.V. Krupskaya) on a D-Max-2000 (Rigaku) diffractometer. The felty masses on rutile crystals and the precipitate from the ampoule were determined to contain two TiO_2 modifications and the $Na_2Ti_6O_{13}$, $TiCl_3$, and TiOCl Ti-bearing phases (the three latter phases obviously contain trivalent Ti). Conceivably, the amount of the newly formed phase was so low that did not any perceptibly modify the Ti concentration of the aqueous solution. Our results obtained on the Ti concentrations depending on the NaOH concentration generally demonstrate a clearly pronounced rectilinear dependence.

By analogy with the complexation of other fourth-group elements (Sn and Zr), rutile dissolution in NaOH solutions can be described by the reaction of OH^- addition

$$TiO_2(\text{rutile}) + nOH^- = Ti(OH)_4(OH)_n^{n-}. \qquad (4)$$

In considering the calculated constants of equilibrium (4), the constant in Table 11 does not change for the complex $Ti(OH)_6^{2-}$ at NaOH concentrations of 0.1–0.5 m, i.e., at $n = 2$ ($K = 0.0343$, $pK = 1.46$). Assuming

Table 9. Calculation of the constant of the equilibrium TiO_2(rutile) + nH^+ + $nHSO_4^-$ = $Ti(OH)_{4-2n}(SO_4)_n$ + nH_2O at 500°C, 1000 bar, and the Ni/NiO buffer

H_2SO_4 concentration (m)	HSO_4^- and H^+ activities (m)	$\frac{Ti(aq) - Ti(H_2O)}{(HSO_4^-)(H^+)}$ $K \times 10^{-4}$	$\frac{Ti(aq) - Ti(H_2O)}{(HSO_4^-)^2(H^+)^2}$ K	$\frac{Ti(aq) - Ti(H_2O)}{(HSO_4^-)^3(H^+)^3}$ $K \times 10^5$
First approximation				
0.01	0.00248	2950	48100	–
0.1	0.0102	105	101	–
0.2	0.0158	73.5	29.5	1.2
0.3	0.0204	22.5	29.4	0.71
0.4	0.0244	188	31.6	0.53
0.5	0.0282	290	36.5	0.46
Second approximation				
0.1	0.0102	105	–	–
0.2	0.0158	–	–	–
0.3	0.0204	–	29.4	–
0.4	0.0244	–	31.6	–
0.5	0.0282	–	36.5	–

Note: Average values: K = 0.0105, pK = 1.98 for the reaction TiO_2(rutile) + H^+ + HSO_4^- = $Ti(OH)_2SO_4$; K = 32.5, pK = –1.51 for the reaction TiO_2(rutile) + $2H^+$ + $2HSO_4^-$ = $Ti(SO_4)_2$ + $2H_2O$.

that 0.05 m NaOH solution is a boundary solution for equilibria with n = 2 and n = 1, constant (4) of the $Ti(OH)_5^-$ complex should be evaluated in NaOH solutions with concentrations of less than 0.05 m. The range of NaOH concentrations of 0.03–0.1 m displays smaller variations of the constants at n = 1, but this range overlaps with the range of 0.1–0.5 m NaOH for n = 2. Thus, we were forced to conduct the calculations at 0.05–0.03 m NaOH ($K = 6.76 \times 10^{-4}$, pK = 3.17). The OH^- activity in the NaOH solution at 500°C and 1000 bar was calculated by the HCh computer program. The activity coefficients of the dissolved Ti species were assumed to be equal to one.

System rutile–aqueous NaF solutions (Table 12). The rutile solubility at all of the three buffers at NaF concentrations of <0.274 m completely coincided with the results obtained for HF solutions with the same concentrations (compare Figs. 2 and 7). In solutions with 0.5 and 0.75 m NaF, the rutile solubility was lower than in the corresponding HF solutions and decreased by 0.2 log m Ti(aq) in 1 m NaF solution. The reaction of rutile dissolution in NaF solutions proceeds in alkaline environments, at the predominance of fluoride ions ($F^- > OH^-$) among the ligands (Table 13). Because of this, the reaction of rutile dissolution can be written as

$$TiO_2(\text{rutile}) + 2H_2O + nF^- = Ti(OH)_4F_n^{n-} \ (F^- \text{ addition reaction}), \quad (5)$$

$$TiO_2(\text{rutile}) + 2H_2O + nF^- = Ti(OH)_{4-n}F_n + nOH^- \quad (6)$$

(OH^- substitution for F^-).

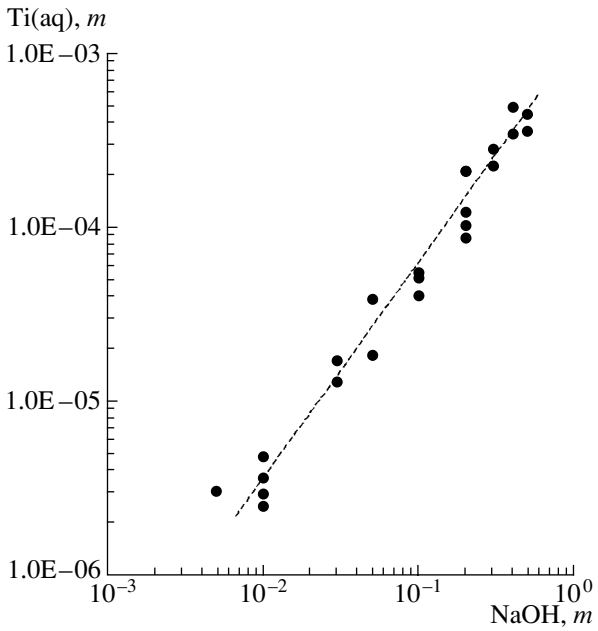

Fig. 5. Rutile solubility in NaOH solutions at 500°C, 1000 bar, and the Ni/NiO buffer.

Table 10. Rutile solubility in NaOH solutions at 500°C, 1000 bar, and the Ni/NiO buffer

Initial NaOH concentration (m)	Experimentally determined value of the Ti concentration ($m \times 10^{-4}$)	Averaged Ti solubility value ($m \times 10^{-4}$)
0.005	0.0308	0.0308
0.01	0.0360	0.0347
	0.0251	
	0.0480	
	0.0297	
0.03	0.170	0.150
	0.129	
0.05	0.182	0.281
	0.380	
0.1	0.518	0.487
	0.403	
	0.540	
0.2	0.862	1.29
	2.05	
	1.21	
	1.02	
0.3	2.22	2.50
	2.77	
0.4	4.82	4.10
	3.37	
0.5	4.41	3.97
	3.52	

In order to rigorously justify the choice between these reaction, one should examine the rutile solubility (i) at constant alkalinity and a varying fluoride concentration and (ii) at a constant fluoride concentration and varying alkalinity. The concentrations of fluoride ions in our experiments were varied more significantly than the concentrations of hydroxide ions (Table 13). The activities of the fluoride and hydroxide ions in the NaF solutions at 500°C and 1000 bar were calculated by the HCh program (Yu.V. Shvarov). The activity coefficient of the dissolved titanium fluoride species was assumed to be equal to one. The independence of the constants of reactions (5) and (6) of the NaF concentration (Table 13) provides a criterion for selecting between them. Preliminary calculations demonstrate that the constants of both reactions do not change, except at the point corresponding to 0.027 m in NaF solution (Table 13), which did not allow us to give preference to either of these constants. However, if these constants are assumed to equally contribute to the dissolved Ti concentration Ti(aq) and the analytically determined Ti(aq) is divided in half, then $K = 2.06 \times 10^{-4}$, p$K = 3.69$ for reaction (5) and $K = 1.37 \times 10^{-6}$, p$K = 5.86$ for reaction (6).

Titanium in thermal waters. Rare analyses of natural waters (Table 14) from thermal springs in volcanic areas in which Ti was detected display a rectilinear dependence of the Ti concentration in the water on the total concentration of $SO_4^{2-} + HSO_4^-$ (Fig. 8) and on the Cl concentration (Fig. 9). Available data indicate that the dependence of the Ti concentration on the concentration of the fluoride ion in thermal waters is pronounced not so clearly.

The proportions of the concentrations of Ti and HSO_4^- and of Ti and Cl^- were utilized to calculate the constants of Eqs. (1) and (3), which are listed in Table 15. The analytical errors involved in the determined HSO_4^-, Cl^-, and H^+ concentrations in thermal waters and the difficulties in relating the measured concentrations to a temperature of 25°C make the recalculations of the concentrations into activities not very reliable.

TITANIUM COMPLEXATION UNDER THE PARAMETERS OF THE HYDROTHERMAL PROCESS

The determination of the constants of equilibria (1)–(6) makes it possible to evaluate the Gibbs free energy (Δg^0) at 500°C and 1000 bar for the following experimentally identified complex species of Ti, $Ti(OH)_3Cl^0$, $Ti(OH)_2Cl_2^0$, $Ti(OH)_2SO_4^0$, $Ti(OH)_5^-$, $Ti(OH)_6^{2-}$, $Ti(OH)_3F^0$, $Ti(OH)_2F_2^0$, and $Ti(OH)_4F^-$, by using the thermodynamic relation

$$-RT\ln K^\circ = \Sigma\ (\Delta g^0 \text{ reaction products} - \Delta g^0 \text{ starting compounds}), \quad (7)$$

and the Δg^0 values for HF^0, HCl^0, H^+, OH^-, HSO_4^-, F^-, and H_2O, which participate in reactions (1)–(6), from the UNITHER database [25]. The values of the Gibbs free energy of the compounds participating in reactions

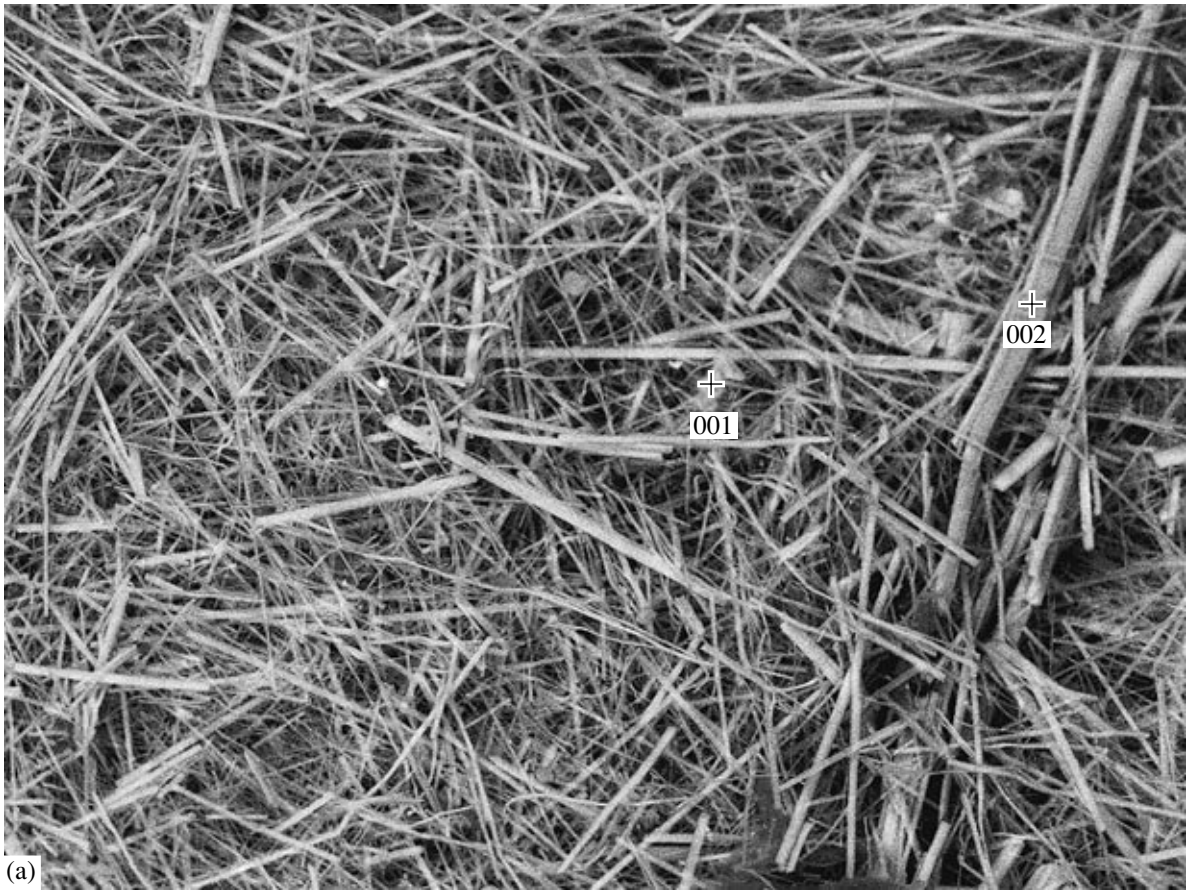

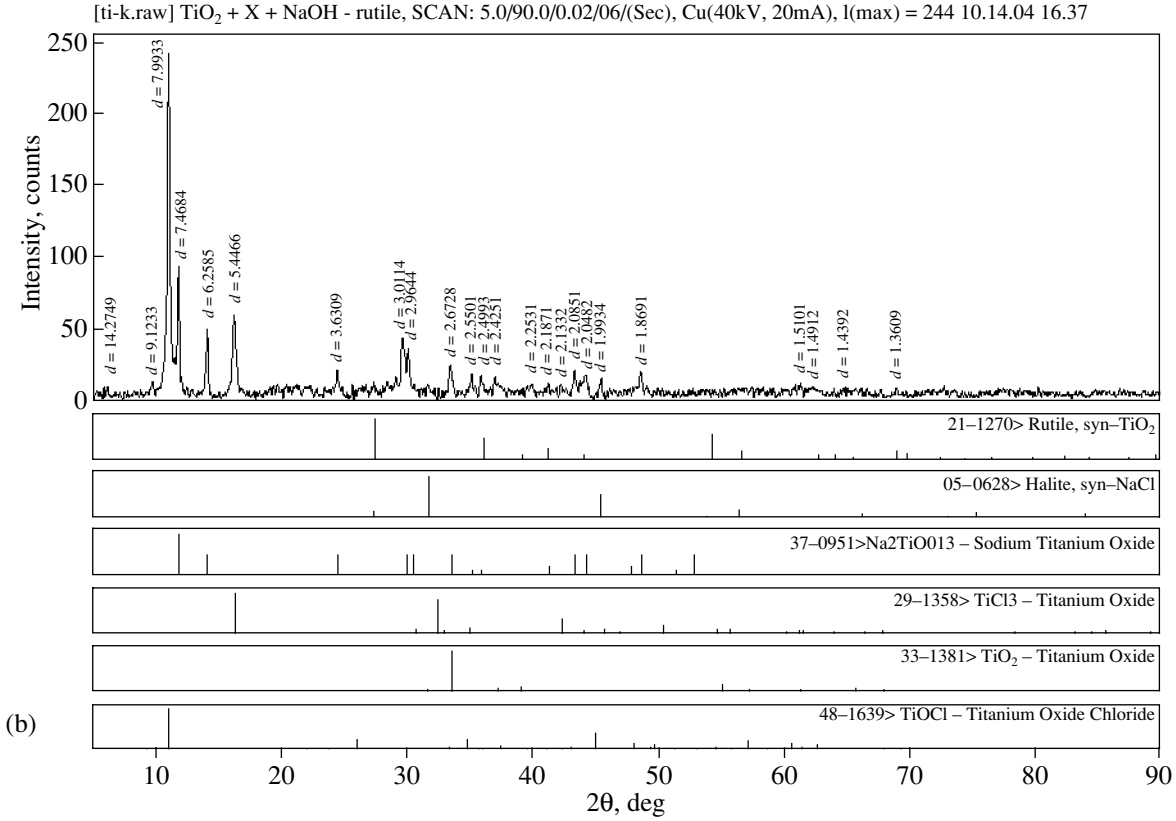

Fig. 6. Newly formed phases on the surface of rutile crystals after the experiments: (a) electron microscope image and (b) spectrum.

Table 11. Calculation of the constant of the equilibrium TiO_2(rutile) + nOH^- = $Ti(OH)_4(OH)_n^{n-}$ at 500°C, 1000 bar, and the Ni/NiO buffer

NaOH concentration (m)	OH^- activity (m)	$\frac{Ti(aq) - Ti(H_2O)}{(OH^-)}$ $K \times 10^{-4}$	$\frac{Ti(aq) - Ti(H_2O)}{(OH^-)^2}$ $K \times 10^{-4}$
First approximation			
0.005	0.00344	6.04	1758
0.0100	0.00598	4.13	691
0.03	0.0139	10.1	725
0.05	0.0206	13.2	639
0.1	0.0351	13.6	387
0.2	0.0607	21.1	347
0.3	0.0842	29.6	351
0.4	0.1067	38.3	359
0.5	0.1205	32.9	273
Second approximation			
0.005	0.00344	6.04	–
0.01	0.00598	4.13	–
0.03	0.0139	10.1	–
0.1	0.0351	–	387
0.2	0.0607	–	347
0.3	0.0842	–	351
0.4	0.1067	–	359
0.5	0.1205	–	273

Note: $K = 6.76 \times 10^{-4}$, pK = 3.17 for the reaction TiO_2(rutile) + OH^- = $Ti(OH)_5^-$; K = 0.0343, pK = 1.46 for the reaction TiO_2(rutile) + $2OH^-$ = $Ti(OH)_6^{2-}$.

Table 12. Rutile solubility ($m \times 10^{-4}$) in NaF solutions at 500°C and 1000 bar

Initial NaF concentration (m)	MnO_2/Mn_2O_3 buffer $fH_2 = 8 \times 10^{-12}$ bar	Ni/NiO buffer fH_2 = 1.74 bar	$Al \longrightarrow Al_2O_3$ fH_2 = 10.3 bar	Averaged Ti concentration ($m \times 10^{-4}$)
0.027	0.026	0.026	0.026	0.026
0.137	0.149	0.270	0.220	0.213
0.274	0.470	0.296	0.602	0.456
0.50	0.606	–	0.387	0.447
0.75	0.993	0.460	0.750	0.734
1.0	0.589	0.580	0.610	0.593

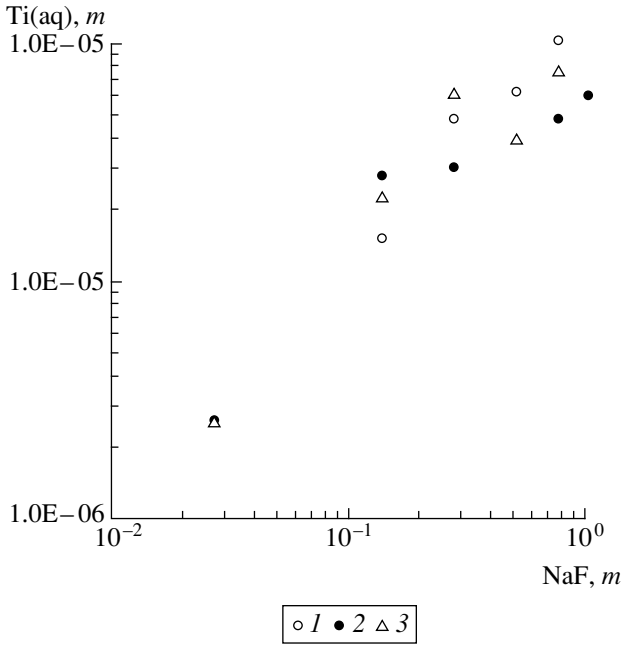

Fig. 7. Rutile solubility in NaF solutions at 500°C, 1000 bar, and the (1) MnO_2/Mn_2O_3, (2) Ni/NiO, and (3) Al ⟶ Al_2O_3 buffers.

(1)–(6) and the calculated Gibbs free energy for $Ti(OH)_2Cl_2^0$, $Ti(OH)_3Cl^0$, $Ti(OH)_2F_2^0$, $Ti(OH)_3F^0$, $Ti(OH)_4F^-$, $Ti(OH)_2SO_4^0$, and $Ti(SO_4)_2^0$ are listed in Table 16.

The determination of the constants for $Ti(OH)_3Cl^0$ and $Ti(OH)_2SO_4^0$ at 25°C from the composition of volcanic emanations allowed us to correlate the results of our experimental research at 500°C and 1000 bar with

Table 13. Calculation of the constant of the equilibria TiO_2(rutile) + $2H_2O$ + nF^- = $Ti(OH)_4F_n^{n-}$ (reaction of F^- addition) and TiO_2(rutile) + $2H_2O$ + nF^- = $Ti(OH)_{4-n}F_n$ + nOH^- (reaction of OH^- substitution for F^-) at 500°C and 1000 bar

Initial NaF concentration (*m*)	F^- activity (*m*)	OH^- activity (*m*)	$\frac{Ti(aq) - Ti(H_2O)}{F^-}$ $K \times 10^{-4}$	$\frac{[Ti(aq) - Ti(H_2O)] \cdot OH^-}{F^-}$ $K \times 10^{-6}$
First approximation				
0.027	0.0104	0.00278	1.54	0.428
0.137	0.0421	0.00463	4.82	2.23
0.274	0.0760	0.00581	5.87	3.41
0.50	0.128	0.00715	3.41	2.44
0.75	0.182	0.00830	3.98	3.30
1.00	0.235	0.00922	2.52	2.33
Second approximation				
0.137	0.0421	0.00463	2.41	1.12
0.274	0.0760	0.00581	2.93	1.70
0.50	0.128	0.00715	1.70	1.22
0.75	0.182	0.00830	1.99	1.65
1.00	0.235	0.00922	1.26	1.17

Note: Reaction (5) TiO_2(rutile) + $2H_2O$ + F^- = $Ti(OH)_4F^-$ (reaction of F^- addition); reaction (6) TiO_2(rutile) + $2H_2O$ + F^- = $Ti(OH)_3F$ + OH^- (reaction of OH^- substitution for F^-). The constancy of the concentration constants of both reactions did not allow us to give preference to any of them. Assuming their equal contributions to the dissolved Ti concentration Ti(aq), we obtained $K = 2.04 \times 10^{-4}$, pK = 3.69 for reaction (5) and $K = 1.37 \times 10^{-6}$, pK = 5.86 for reaction (6).

Table 14. Composition of naturally occurring thermal waters in active volcanic areas [2, 10, 11]

Volcanic mineral-forming solutions	Component concentrations, mg/l				
	Ti (IV)	SO_4^{2-}	HSO_4^-	Cl^-	F^-
Nizhne-Mendeleevskii spring	0.7	1052.1	983.5	1065.0	–
Hydrothermal solution from Mendeleeva volcano	0.0011	1.0041	0.0940	0.0141	–
Hydrothermal solution from Golovina volcano	0.5	475.2	84.3	226.9	–
Spring in the headwaters of the Yur'eva River	0.6	4157.5	4067.2	3304.9	11.25
Mouth of the Yur'eva River	0.08	1707.0	885.3	925.5	0.5
Ebeko volcano, NE fumarole field	4.28	927.0	4189.5	18354.1	6.0
Ebeko volcano, NE fumarole field	0.52	3845.3	3215.9	95.7	5.2
Ebeko volcano, 1st Eastern Cirque	1.68	334.3	995.9	5985.6	8.0
Karan-Idzhen crater lake	23.42	60223.02	–	20561.41	–
Lake in the Trotskii crater	6.9	6347.0	11059.0	8793.3	–

data on the surface *P–T* conditions by using the electrostatic model of electrolyte ionization [25]. The estimates of the temperature functions of dissociation constants are of approximate character. Data on the temperature functions of the analogous species of Sn(IV) were used to assay the constants of the $Ti(OH)_3F^0$, $Ti(OH)_4^0$, $Ti(OH)_5^-$, and $Ti(OH)_6^{2-}$ complexes. The independent tests of the values proposed for the ionization constants of Ti complexes, which were carried out by comparing the calculated and experimentally determined rutile solubilities (Table 1) in 1 M NaCl solution, demonstrate that the calculated values are lower than the experimen-

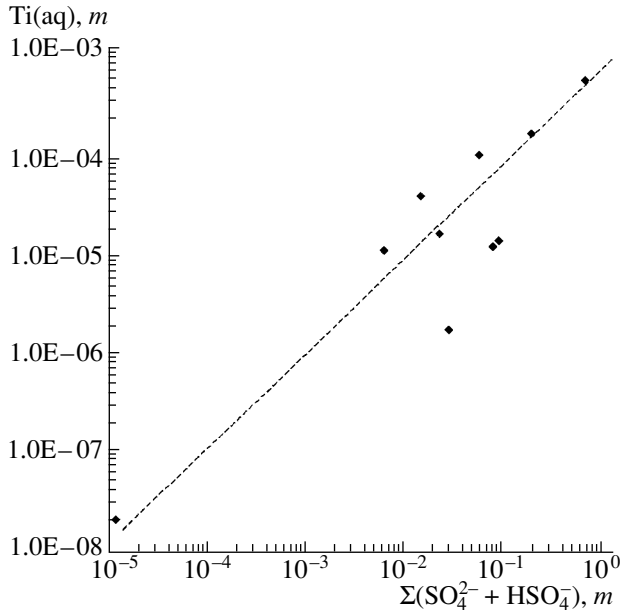

Fig. 8. Dependence of the Ti concentration on the overall concentrations of SO_4 in waters naturally occurring in volcanic areas.

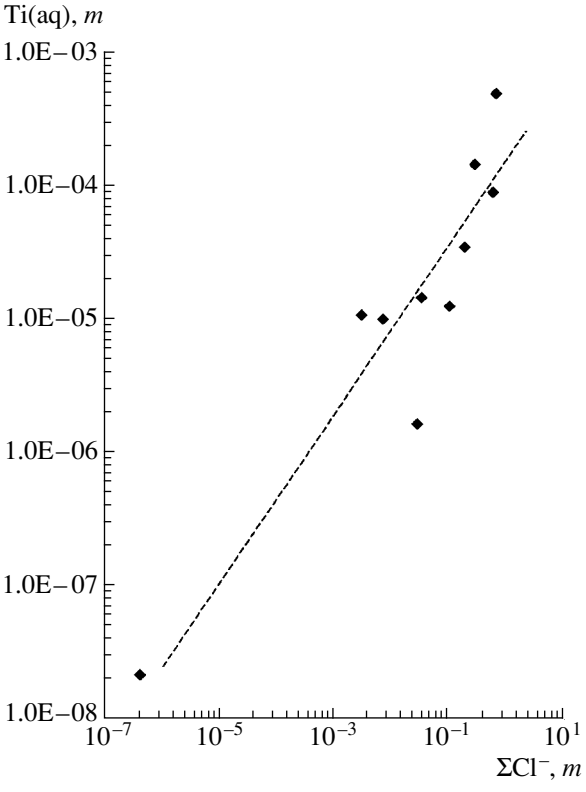

Fig. 9. Dependence of the Ti concentration on the overall concentrations of Cl in waters naturally occurring in volcanic areas.

Table 15. Calculation of the constants of equilibria (1) and (3) at 25°C and 1 bar from the composition of volcanic mineral-forming solutions

Mineral-forming solution	$\log m HSO_4^-$	$\log m Cl^-$	pH	$\log m$Ti(aq)	$\log K_1$	$\log K_3$
Reaction (1) TiO_2(rutile) + H_2O + Cl^- + H^+ = $Ti(OH)_3Cl^0$ $\log K = \log m$Ti(aq) – $\log m Cl^-$ + pH						
Ebeko volcano, NE fumarole field	–	–0.71	0.44	–4.05	–2.90	
Ebeko volcano, 1st Eastern Cirque	–	–0.77	0.91	–4.45	–2.77	
Lake in the Trotskii crater	–	–0.61	0.69	–3.84	–2.54	
Reaction (3) TiO_2(rutile) + HSO_4^- + H^+ = $Ti(OH)_2SO_4^0$ $\log K = \log m$Ti(aq) – $\log m HSO_4^-$ + pH						
Karan-Idzhen crater lake	–0.20	–	0.02	–3.62		–3.40

Table 16. Gibbs free energy (kJ/mol) of components participating in reactions (1)–(6) (according to [25]) and the results of this research

Component	25°C, 1 bar	500°C, 1 kbar	Component	25°C, 1 bar	500°C, 1 kbar
TiO_2(rutile)	–888.951	–927.068	$Ti(OH)_3Cl^0$	–1237.653	–1314.210
H_2O	–237.141	–287.953	$Ti(OH)_2Cl_2^0$	–	–1200.086
H^+	0	0	$Ti(OH)_3F^0$	–1419.222	–1546.189
OH^-	–157.262	–112.991	$Ti(OH)_2F_2^0$	–	–1547.510
HCl^0	–127.240	–171.221	$Ti(OH)_4F^-$	–	–1691.672
HF^0	–299.834	–376.756	$Ti(OH)_2SO_4^0$	–1623.353	–1703.384
Cl^-	–131.290	–117.712	$Ti(SO_4)_2^0$	–	–1984.767
F^-	–299.845	–243.317	$Ti(OH)_4^0$	–1323.274	–1414.297
HSO_4^-	–755.756	–805.626	$Ti(OH)_5^-$	–1457.876	–1569.074
SO_4^{2-}	–774.459	–679.554	$Ti(OH)_6^{2-}$	–1614.110	–1707.380

tal ones. For example, the experimental solubility at 200°C and the saturation vapor pressure of water is equal to 2.8×10^{-5} *m*, and the corresponding calculated values are 4×10^{-6} *m* (under saturated vapor pressure) and 2×10^{-5} *m* (under a pressure of 1000 bar). The experimental value at 300°C is 3.3×10^{-5} *m* (under water saturation vapor pressure), whereas the calculated values are equal to 3×10^{-6} *m* (under saturated vapor pressure) and 1×10^{-5} (under a pressure of 1000 bar).

Although our values for the Gibbs free energy of the aforementioned Ti complexes are of approximate character, they allowed us to calculate the solubility of TiO_2 (rutile) in high-temperature postmagmatic fluids. Both

Table 17. Limiting Ti(aq) concentrations in a hydrothermal fluid of the composition (1 *m* F + 1 *m* Cl + 1 *m* SO_4 + Na) at various pH values

500°C, 1000 bar		400°C 750 bar		200°C, 250 bar	
pH	Ti(aq), *m*	pH	Ti(aq), *m*	pH	Ti(aq), *m*
2.0	1.4×10^{-4}	1.5	6.6×10^{-4}	2.2	6.4×10^{-3}
5.0	1.2×10^{-4}	6.0	3.1×10^{-4}	4.0	4.4×10^{-3}
7.5	7.2×10^{-5}	8.0	1.8×10^{-5}	7.0	1.6×10^{-5}
9.5	2.1×10^{-4}	9.5	6.1×10^{-5}	10	6.0×10^{-6}

the results of the direct determination of the rutile solubility in aqueous solutions of variable composition at 500°C and 1000 bar (Tables 1, 3, 5, 8, 10, 12) and the results of our model simulations (Table 17) testify that the mobility of Ti in aqueous fluids during postmagmatic processes is low and increases only in F-rich and acid solutions.

ACKNOWLEDGMENTS

This study was supported by the Russian Foundation for Basic Research, project no. 02-05-65003.

REFERENCES

1. B. V. Nekrasov, *Course of General Chemistry* (Goskhimizdat, Moscow, 1962) [in Russian].
2. B. V. Chesnokov, "Trivalent Titanium in Eclogites of the Southern Urals," Geokhimiya, No. 1, 68–71 (1960).
3. Ya. G. Goroshchenko, *Titanium Chemistry* (Naukova Dumka, Kiev, 1970) [in Russian].
4. V. V. Shcherbina, "On the Geochemistry of Titanium," Geokhimiya, No. 3, 302–309 (1971).
5. I. V. Veksler and M. P. Tenteleev, "Titanium Geochemistry in Alkaline Magmatic Systems based on Experimental Study of Nepheline–Diopside–Titanite System," Geokhimiya, No. 5, 642–651 (1991).
6. *Genesis of Endogenous Ore Deposits,* Ed. by V. I. Smirnov (Nedra, Moscow, 1968) [in Russian].
7. V. G. Krivovichev, "Thermodynamics of Equilibria of Fe and Ti Minerals during Hydrothermal Metasomatism," in *Proceedings of Symposium on Thermodynamics in Geology, Suzdal, Russia, 1985* (Suzdal, 1985), p. 204 [in Russian].
8. S. R. Krainov, *Geochemistry of Trace Elements in Underground Waters* (Nedra, Moscow, 1973) [in Russian].
9. S. I. Naboko, *Hydrothermal Metamorphism of Rocks in Volcanic Areas* (Akad. Nauk SSSR, Moscow, 1963) [in Russian].
10. B. V. Ivanov, "Modern Hydrothermal Activity in the Area of the Karymskii Volcanic Group," in *Hydrothermal Mineral-Forming Solutions in the Areas of Active Volcanism* (Nauka, Novosibirsk, 1974), pp. 32–38 [in Russian].
11. I. A. Menyailov and L. P. Nikitina, "Zinc and Lead in the Gases and Waters of Ebeko Volcano and the Pauzhetka Deposit," in *Hydrothermal Mineral-Forming Solutions in the Areas of Active Volcanism* (Nauka, Novosibirsk, 1974), pp. 103–110 [in Russian].
12. G. F. Agapova, I. S. Modinkov, and E. M. Shmariovich, "Experimental Study of Titanium Behavior in Thermal Sulfide–Carbonate Solutions," Geol. Rudn. Mestorozhd., No. 2, 73–79 (1989).
13. M. L. Barsukova, V. A. Kuznetsov, V. A. Dorofeeva, and I. L. Khodakovskii, "Experimental Study of the Solubility of Rutile TiO_2 in Fluid Solutions at High Temperatures," Geokhimiya, No. 7, 1017–1027 (1979).
14. A. L. Kotel'nikova and V. K. Purtov, *Study of the Solubility of Synthetic Rutile in Water and HF and HCl Aqueous Solutions at 473–973 K and 1 kbar. Year Book 1992* (Zavaritskii Inst. Geol. Geokhim., Yekaterinburg, 1993) [in Russian].
15. V. K. Purtov and A. L. Kotel'nikova, "On the Migration Properties of Titanium in Chloride and Fluoride Hydrothermal Solutions Based on Experimental Data," Geol. Rudn Mestorozhd. **34** (6), 61–69 (1992).
16. R. D. Shuilling and B. W. Vink, "Stability Relations of Some Titanium Minerals (Sphene, Perovskite, Rutile, Anatase)," Geochim. Cosmochim. Acta **31**, 2399–2411 (1967).
17. J. C. Ayers and E. B. Watson, "Solubility of Apatite, Monazite, Zircon and Rutile in Supercritical Aqueous Fluids with Implications for Subduction Zone Geochemistry," Philos. Trans. Royal Soc. London, Ser A. **335**, 365–375 (1991).
18. J. C. Ayers and E. B. Watson, "Rutile Solubility and Mobility in Supercritical Fluids," Contrib. Mineral. Petrol. **114**, 321–330 (1993).
19. V. A. Kuznetsov and V. V. Panteleev, "Hydrothermal Synthesis of Rutile," Kristallografiya **10**, 445 (1965).

20. V. A. Kuznetsov, "Crystallization of Oxides of the Ti-Subgroup Metals," in *Study of Crystallization under Hydrothermal Conditions* (Nauka, Moscow, 1970), pp. 43–54 [in Russian].

21. L. N. Dem'yanets, "Hydrothermal Synthesis of Oxides of Transition Metals," in *Hydrothermal Synthesis and Growing of Monocrystals* (Nauka, Moscow, 1982), pp. 16–17 [in Russian].

22. I. N. Anikin and G. V. Rumyantseva, "On the Solubility and Recrystallization of TiO_2 under Hydrothermal Conditions," in *Study of Natural and Technical Mineral Fomation* (Moscow, 1966), pp. 277–279 [in Russian].

23. L. P. Nikitina and N. N. Basargin, "New Method of Photometrical Determination of Titanium (IV) in Natural Waters," Zh. Anal. Khim., No. 8, 1521–1523 (1970).

24. N. N. Basargin and A. V. Lebedkova, "Photometrical Determination of Low Titanium Contents in Ultramafic Rocks and Minerals by Tichromine," in *Chemical and Physicochemical Methods of Analysis of Ores, Rocks, and Minerals* (Nauka, Moscow, 1974), pp. 41–44 [in Russian].

25. M. V. Borisov and Yu. V. Shvarov, *Thermodynamics of Geochemical Processes* (Mosk. Gos. Univ., Moscow, 1992) [in Russian].